viruses

MDPI

Article

The *Petasites hybridus* CO_2 Extract (Ze 339) Blocks SARS-CoV-2 Replication In Vitro

Lorena Urda [1], Matthias Heinrich Kreuter [2], Jürgen Drewe [2], Georg Boonen [2], Veronika Butterweck [2,*] and Thomas Klimkait [1,*]

[1] Department Biomedicine, University of Basel, Petersplatz 10, 4051 Basel, Switzerland; lorena.urda@unibas.ch
[2] Medical Department, Max Zeller & Söhne AG, Seeblickstrasse 4, 8590 Romanshorn, Switzerland; matthias.kreuter@zellerag.ch (M.H.K.); juergen.drewe@zellerag.ch (J.D.); georg.boonen@zellerag.ch (G.B.)
* Correspondence: veronika.butterweck@zellerag.ch (V.B.); thomas.klimkait@unibas.ch (T.K.); Tel.: +41-71-4660447 (V.B.); +41-61-2073272 (T.K.)

Abstract: The coronavirus disease 2019 (COVID-19), caused by a novel coronavirus (SARS-CoV-2), has spread worldwide, affecting over 250 million people and resulting in over five million deaths. Antivirals that are effective are still limited. The antiviral activities of the *Petasites hybdridus* CO_2 extract Ze 339 were previously reported. Thus, to assess the anti-SARS-CoV-2 activity of Ze 339 as well as isopetasin and neopetasin as major active compounds, a CPE and plaque reduction assay in Vero E6 cells was used for viral output. Antiviral effects were tested using the original virus (Wuhan) and the Delta variant of SARS-CoV-2. The antiviral drug remdesivir was used as control. Pre-treatment with Ze 339 in SARS-CoV-2-infected Vero E6 cells with either virus variant significantly inhibited virus replication with IC_{50} values of 0.10 and 0.40 µg/mL, respectively. The IC_{50} values obtained for isopetasin ranged between 0.37 and 0.88 µM for both virus variants, and that of remdesivir ranged between 1.53 and 2.37 µM. In conclusion, Ze 339 as well as the petasins potently inhibited SARS-CoV-2 replication in vitro of the Wuhan and Delta variants. Since time is of essence in finding effective treatments, clinical studies will have to demonstrate if Ze339 can become a therapeutic option to treat SARS-CoV-2 infections.

Keywords: SARS-CoV-2; COVID-19; anti-COVID-19; antiviral; Delta variant; *Petasites hybridus*; isopetasin; cytotoxicity; selectivity index

Citation: Urda, L.; Kreuter, M.H.; Drewe, J.; Boonen, G.; Butterweck, V.; Klimkait, T. The *Petasites hybridus* CO_2 Extract (Ze 339) Blocks SARS-CoV-2 Replication In Vitro. *Viruses* **2022**, *14*, 106. https://doi.org/10.3390/v14010106

Academic Editors: Luis Martinez-Sobrido and Fernando Almazan Toral

Received: 2 December 2021
Accepted: 5 January 2022
Published: 7 January 2022

1. Introduction

COVID-19 (coronavirus disease 2019) first appeared in China at the end of 2019 and has, since then, spread around the globe, causing more than 5 million deaths [1]. Severe acute respiratory syndrome coronavirus-2 (SARS-CoV-2) is transmitted mainly via droplets and aerosols (for review see [2]). Infectivity begins one to several days before symptom onset, and even asymptomatically infected individuals can transmit the virus [2]. The disease affects the upper respiratory tract and lungs, heart, liver, gastrointestinal tract, and other organs, but the majority of infections remains asymptomatic, and patients develop only mild symptoms [3]. However, severe courses of COVID-19 are commonly accompanied by severe immune activation [4]. Observations include lymphocytopenia; an increase in neutrophils; and increased serum levels of IL-1β, IL-2, IL-4, IL-6, IL-10, TNF-α, and interferon-γ [3,5,6]. This cytokine response (also referred to as 'cytokine storm') is associated with cellular injury, which in turn is reflected in increased serum levels of lactate dehydrogenase (LDH), cardiac and hepatic enzymes, and the activation of coagulation and fibrinolysis with markedly increased plasma levels of D-dimers, among others [3,5,6]. In acute respiratory distress syndrome (ARDS) due to COVID-19, alveolar injury with desquamation of pneumocytes, hyaline membranes, and lymphomonocytic infiltrates has been described [7–9]. Lymphocytic endothelitis and apoptosis of endothelial cells in lungs, kidneys, and small intestine have also been observed [10]. The hyperinflammatory host response caused by an overproduction

of early-response proinflammatory cytokines (e.g., TNFα, IL-6, IL1-ß) leads to multiorgan thrombotic complications, hyperpermeability, organ failure, and death [11,12]. For severe cases, several therapeutic strategies to target the hyperinflammation caused by an overactive cytokine response are currently being explored (for review see [13]).

However, a breakthrough in drug therapy has not yet been achieved, although the first candidates for an oral therapy have reached the approval process [14]. Among those is Paxlovid™ with the active ingredient PF-07321332, which is the first oral antiviral drug available to combat SARS-CoV-2. PF-07321332 is an antiviral medication developed by Pfizer that inhibits the activity of 3C-like protease ($3CL^{PRO}$) required for virus replication. Without the activity of the SARS-CoV-2 $3CL^{PRO}$, nonstructural proteins (including proteases) cannot be released to perform their functions, thereby inhibiting viral replication [15]. Paxlovid™ also contains a modest dose of ritonavir (a Ser-protease inhibitor and inhibitor of cytochrome P450 3A4), which delays the breakdown of PF-07321332, allowing it to stay in the body for longer at virus-inhibiting levels. In COVID-19 patients, the drug is likely to lower the rates of hospitalization [16]. Another drug currently under investigation is Molnupiravir, a Ridgeback Biotherapeutics product licensed by Merck, which increases the frequency of spontaneous alterations in the viral RNA and, thus, inhibits SARS-CoV-2 replication [14].

In the numerous clinical trials that are currently being conducted worldwide, only remdesivir and dexamethasone have shown partial efficacy in combating hyperinflammatory stages of severe COVID-19 [17–24]. Furthermore, monoclonal antibodies, which block coronavirus surface proteins and reduce SARS-CoV-2 infection, are the only type of therapy approved in the United States for early-stage COVID-19. However, the high cost (about USD 2000 per dose, currently subsidized by the federal government in the United States), scarcity, and necessity to infuse or inject them have hindered their usage, especially in the developing world [14]. Therefore, COVID-19 therapies that are both affordable and simple to use are critically needed.

Recent studies suggest that, in addition to cytokines, leukotrienes (LTs) could also be considered as therapeutic targets since they further contribute to hyperinflammation in severe COVID-19 cases [25–29]. The involvement of LTs in severe COVID-19 cases has been shown in some recent studies, confirming high LT levels in the bronchoalveolar lavage fluid of COVID-19 patients [30,31].

Leukotrienes (LTB_4, LTC_4, LTD_4, and LTE_4) are peptide-conjugated lipids that are prominent products of activated eosinophils, basophils, mast cells, and macrophages [32–34]. They are generated de novo from cell membrane phospholipid-associated arachidonic acid via the 5-lipoxygenase pathway. Known to cause contraction of bronchial smooth muscle, leukotrienes have been recognized as potent inflammatory mediators that initiate and propagate a diverse array of biologic responses, including macrophage activation, mast cell cytokine secretion, and dendritic cell maturation and migration [35,36]. Thus, it is likely that LTs could play an important role in the hyperimmune/inflammatory storm observed in COVID-19 [29]. It has been proposed recently that montelukast, a leukotriene receptor antagonist, and zileuton, a 5-lipoxygenase inhibitor, might be possible treatment options for mild or even severe stages of COVID-19 [25–29], especially when given in combination [27].

Ze 339, a lipophilic subcritical CO_2 extract prepared from the leaves of *Petasites hybridus* (L.) P.G. Gaertn., B Mey., and Scherb (Asteraceae), is a herbal treatment licensed in Switzerland and other countries used to treat allergic rhinitis [37]. Ze 339 has been demonstrated to inhibit leukotriene synthesis in various in vitro and ex vivo studies; the inhibition was solely attributable to the sum of petasins [38–41]. In particular, in human macrophages activated with platelet-activating factor (PAF), Ze 339 blocked Cys-LT and LTB4 synthesis, and further decreased PAF and complement peptide C5a-mediated Cys-LT synthesis in eosinophils and LTB4 synthesis in neutrophils. In human eosinophils and neutrophils, the effects of the positive control zileuton, an orally active inhibitor of LT production, were similar to Ze 339 [40]. Furthermore, petasin and its isomers exhibited no differences in their ability to inhibit 5-lipoxygenase (5-LOX), leukotriene C4 (LTC4) synthase, and leukotriene A4 (LTA4) hydrolase, according to a recent study [38]. The authors of this study also showed that the extract matrix had no influence on the leukotriene inhibitory effects of

the petasins. In addition to these mechanistic in vitro data, leukotriene levels decreased significantly in nasal lavage fluids of patients suffering from allergic rhinitis after 5 days of oral treatment with Ze 339 [39]. It is noteworthy to mention that Ze 339 also inhibited a pro-inflammatory cytokine and chemokine response in human nasal epithelial cells after stimulation with viral mimics [42]. The authors also showed that the pro-inflammatory cytokine/chemokine response to bacteria was not inhibited by Ze 339. These findings highlight the potential of Ze 339 as a promising candidate for the treatment of a virally induced exacerbation of inflammatory processes in the upper airways.

Based on the findings mentioned above, it was the aim of the present proof-of-concept study to investigate if Ze 339 would also have an impact on SARS-CoV-2 replication in vitro. A cellular infection system was used to assess the ability of the substance(s) to interfere with cellular responses after infection with SARS-CoV-2 virus variants.

2. Materials and Methods

2.1. Compounds and Extract

Ze 339 is a subcritical CO_2 extract prepared from the leaves of *P. hybridus* (drug-extract ratio 50–100:1) and was manufactured by Max Zeller Söhne AG, Romanshorn, Switzerland using a patented procedure [43,44]. One coated film tablet contains 17–40 mg of Ze 339 and is standardized to 8 mg petasins. The herein used Ze 339 batch 150056 contained 37.7% total petasins and 27.2% fatty acids. The remaining 35.1% contained other constituents, such as essential oils, sterols, minerals, and vitamins. Pyrrolizidine alkaloids were quantitatively removed in the manufacturing process using online adsorption technology and were no longer detectable (limit of quantification < 2 ppb). A characteristic GC chromatogram is shown in Supporting Figure S1. The extract was dissolved in a mixture of DMSO–H_2O (50:50), and a stock solution of 2 mg/mL was prepared and further diluted with assay buffer (DMEM, 2% FBS, 1% PS) to the final concentrations between 0.001–20 µg/mL. Petasin (purity 92.82%), neopetasin (purity 94.49%), and isopetasin (purity 96.23%) were purchased from HWI Pharma Services GmbH, Ruelzheim, Germany. Stock solutions of petasin, isopetasin, and neopetasin (10 mg/mL, respectively) were prepared using a DMSO–H_2O (90:10) mixture and further diluted with assay buffer (DMEM, 2% FBS, 1% PS) to reach the final concentrations for testing (0.001–20 µg/mL, corresponding to 3.16–63 µM).

Remdesivir (purity $\geq$ 98%) was purchased from Adipogen AG, Liestal, Switzerland. A 500 µM stock solution was prepared and further diluted with assay buffer to the desired concentrations (0.002–50 µM). To avoid cytotoxicity, the final DMSO concentration in all cellular experiments did not exceed 0.5%

2.2. Cells

Vero E6 cells were provided by the group of V. Thiel, Berne, Switzerland. Cells were cultivated in DMEM, high-glucose media (Gibco, Thermofisher AG, Allschwil, CH, Switzerland), and were supplemented with Pen/Strep (1%, Bioconcept, Allschwil, CH, Switzerland) and 2% fetal bovine serum (FBS, Gibco, Thermofisher) at 37 °C in a humidified atmosphere with 5% CO_2.

2.3. Viral Reconstitution

Virus stocks of the initial Wuhan strain of SARS-CoV-2 were provided by G. Kochs, University of Freiburg, D, (SARS-CoV_FR-3) and by EVAglobal virus archive (SARS-CoV-2 strain/NL/2020—AMS). Virus stocks were propagated in a Biosafety level 3 facility by infecting Vero E6 cells at a multiplicity of 0.1 and harvesting culture supernatant on day 3. The cell-free virus in culture supernatant was quantified by RT-PCR of the S-gene RDB region [45] and by plaque titration. Viral titers were determined by plaque assays in Vero cells.

2.4. Plaque Assay Protocol

Antiviral activity was determined by the degree of inhibition of viral cytopathic effect (CPE). Briefly, Vero E6 cells were seeded at a density of 3×10^6 cells/96-well plate (ca.

3×10^4 per well) one day before infection. On the day of infection, cells (ca. 80% confluent) were incubated with the compound of interest in the above-mentioned concentration range to a layer of uninfected cells. After 2 h of incubating cells with the compound at 37 °C in a humidified CO_2 atmosphere, cells were infected with the virus with 100 plaque-forming units (pfu) per well to assess the inhibitory effects on virus propagation. One hour post viral infection, cultures were overlayed with 100 µL low-melting agarose. Agarose (Bio-Rad Europe GmbH, Basel, CH, Switzerland), in DMEM/2% FBS was heated to melt and then cooled in a waterbath to a temperature of <40 °C, and used to overlay cells in the pre-seeded, infected culture. Then, cells were incubated at 37 °C for approx. 48 h, within which a virus-driven CPE plaque formation is routinely observed in untreated controls. For virus inactivation, 80 µL of formaldehyde (15% *w*/*v*) was added for 10 min to the cultures without removing the low-melting agarose. After this period, fixative, culture medium, and agarose were aspirated, and crystal violet (0.1% *w*/*v*) (Sigma-Aldrich, Buchs, Switzerland) was added to each well and incubated for 5 min. Afterwards, the fixed and stained plates were gently rinsed several times under tap water and dried prior to enumeration. Antiviral activity was determined by the degree of inhibition of viral cytopathic effect (CPE), which became apparent in the form of distinct plaques forming in the cell layer. As the number of plaques observed per well was not easily distinguishable by eye, plates were scanned, and the images were counted as described by Honko et al. [46] using Image J 1.53k software [47]. For image processing, images were made binary images according to the Image J definition, the limit to threshold option was enabled under 'set measurements', and pixels of the selected area were counted. The results were normalized to positive (virus infected) and negative (uninfected cells) controls in each assay plate.

2.5. Cytotoxicity Testing

Vero E6 cells were plated as described above, and 3×10^4/well in 50 µL of complete culture medium/2% FBS was cultured overnight. The drug of interest (stock solution) was diluted in DMEM, supplemented with 2% FBS, and 50 µL was then added per well (in duplicates or triplicates at the indicated final concentration). Then, 100 µL of media was added instead of agarose to reach a final volume of 200 µL/well comparable to the screening plates. The plates were cultured for 48 h, similar to the duration of the infections, after which they were fixed and stained with crystal violet as described above. Cytotoxic effects were evaluated using Image J, as described above.

2.6. Statistics

Compounds were tested in duplicates or triplicates per experiment, and each experiment was repeated at least twice. Antiviral data were fitted to a sigmoidal curve, and a four parameter logistic model was used to calculate IC_{50} values using the equation: Y = Bottom + (Top − Bottom)/(1 + 10^((LogIC50-X) × HillSlope)). The IC_{50} values are reported at 95% confidence intervals. This analysis was performed using GraphPad Prism v.9.2.0 (San Diego, CA, USA).

3. Results

3.1. Inhibition Assay of Remdesivir, Ze 339, Petasin, Isopetasin and Neopetasin against the Original SARS-CoV-2 Wuhan Variant

In this study, the potent antiviral effects of the *Petasites hybridus* CO_2 extract, Ze 339, as well as its active compounds, isopetasin and neopetasin (Figure 1), against SARS-CoV-2 infection of the Vero E6 cell line (derived from primary embryonic monkey kidney epithelial cells) were demonstrated.

The antiviral activity of the test compounds was assessed, as previously described [46,48] by visualization of the extent of the cytopathogenic effect (CPE) in the form of cytolytic plaque formation on Vero E6 cells when infected with a clinical strain of SARS-CoV-2, Wuhan. Vero E6 cells are stable cell lines that express a high level of the ACE2 receptor [49]. They were recently employed in studies to assess SARS-CoV-2 infection and replication by

quantifying the virally induced CPE, leading to the formation of cytolytic plaques [50–53]. Prior to antiviral testing the cytotoxicity of all samples towards Vero E6 cells, 50% cytotoxic concentration (CC_{50}) of the test compounds was determined. In addition, a selectivity index (SI) was determined as CC_{50}/IC_{50}.

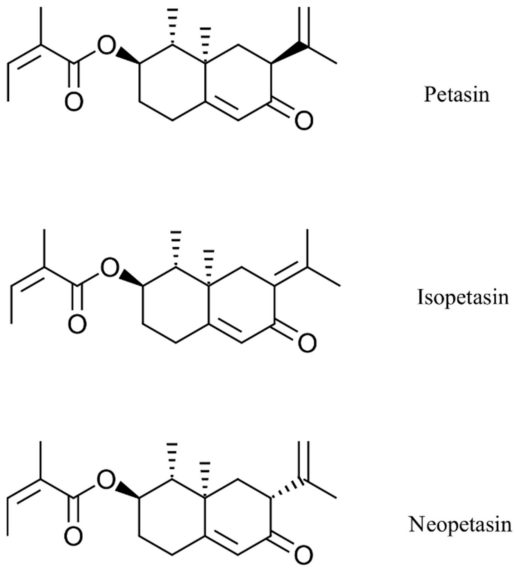

Figure 1. Chemical structures of the main petasins from *Petasites hybridus*.

As shown in Figures 2 and 3, Ze 339, as well as petasin, isopetasin, and neopetasin, did not show any cytotoxic effect in this assay format up to concentrations of 20 µg/mL (63.2 µM for the petasines, respectively).

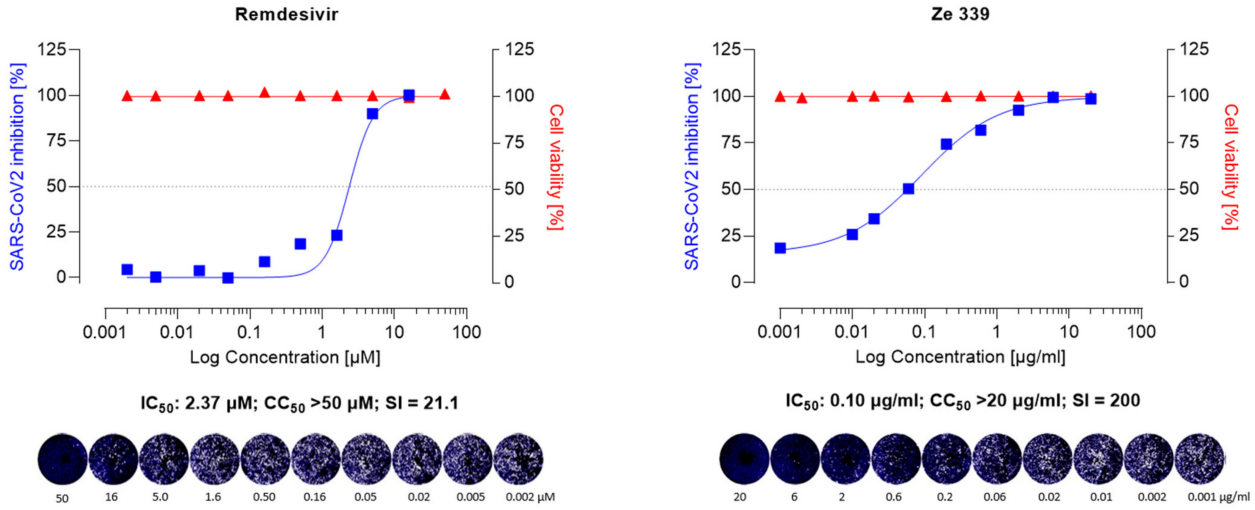

Figure 2. Anti-SARS-CoV-2 activity of the remdesivir and Ze 339 in VeroE6 cells was assessed using the Wuhan strain of SARS-CoV-2. Cells were infected with 100 pfu of a clinical virus isolate in the presence of the indicated concentrations. Blue squares represent inhibition of SARS-CoV-2 infection (%) and red triangles represent cell viability (%). Data are expressed as the mean of two replicates (infection performed in duplicate) with their respected 95% confidence interval. Remdesivir 95% confidence interval = 0.25–0.51, goodness of fit = 0.9668; Ze 339 95% confidence interval = 0.06–0.12, goodness of fit = 0.9962.

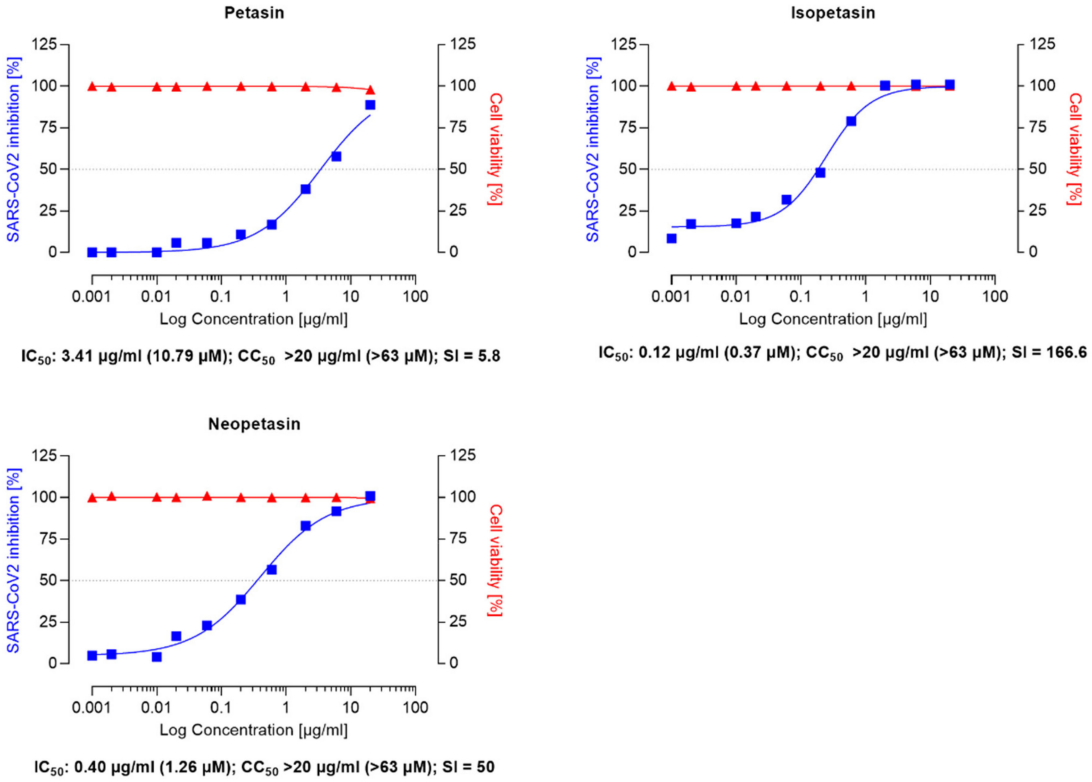

Figure 3. Anti-SARS-CoV-2 activity of the isopetasin and neopetasin in VeroE6 cells was assessed using the Wuhan strain of SARS-CoV-2. Cells were infected with 100 pfu of a clinical virus isolate in the presence of the indicated concentrations. Blue squares represent inhibition of SARS-CoV-2 infection (%), and red triangles represent cell viability (%). Data are expressed as the mean of two replicates (performed in duplicate) with their respected 95% confidence interval. Petasin confidence interval = 2.70–4.31, goodness of fit = 0.9874; Isopetasin 95% confidence interval = 0.15–0.41, goodness of fit = 0.9918; neopetasin 95% confidence interval = 0.27–0.55, goodness of fit = 0.9929.

To investigate whether the *P. hybridus* CO_2 extract Ze 339 and its main active components (petasin, isopetasin, and neopetasin) exert antiviral activity, Vero E6 cells, infected with the Wuhan variant of SARS-CoV-2 were incubated for 48 h in the presence of Ze 339 (0.001–20 µg/mL) or the petasines (0.001–20 µg/mL, corresponding to 0.0031–63.2 µM), respectively. The results demonstrated that Ze 339 (Figure 2) inhibited the formation of virus-driven cytopathic changes in a dose-dependent manner in infected Vero E6 cells with an IC_{50} of 0.12 µg/mL (C.I. 0.06–0.12). The antiviral drug remdesivir was used as reference and showed anti-SARS-CoV-2 activity with an IC_{50} of 2.37 µM (C.I. 0.25–0.51) (Figure 2).

Similar IC_{50} values ranging between 1–11 µM for remdesivir have been reported in the literature [51,52,54]. Compared to remdesivir, isopetasin and neopetasin also exerted potent antiviral activities with IC_{50} values ranging from 0.79–1.2 µM (Figure 3). For petasin, an IC_{50} of 10.79 µM was determined, which was higher than that of isopetasin and neopetasin. According to a recent screening of 5632 compounds (natural products as well as synthetics), including 3488 compounds that underwent clinical stage testing across 600 indications, only 19 compounds were identified as having an IC_{50} in the nanomolar (<1 µM) range, when tested against SARS-CoV-2 in Caco-2 cells [55]. Among those compounds tested were nafamostat and camostat which have different mechanisms of antiviral action [55]. The potent anti-SARS-CoV-2 activity of isopetasin and neopetasin is, therefore, promising. However, further steps are necessary to evaluate the precise underlying mechanism of the antiviral action.

The selectivity index (SI) of a compound is a commonly used metric to express a compound's in vitro efficacy in inhibiting virus reproduction and an important measure to compare the antiviral efficacy of experimental drugs [56]. The greater the SI ratio, the

more successful and safe a medicine should be for treating a viral infection in vivo. The ideal medicine would be cytotoxic at high doses but antiviral at very low concentrations, resulting in a high SI value and the ability to remove the target virus at concentrations much below its cytotoxic concentration.

In our study, Ze 339 showed an SI of 200, compared to an SI of 21.1 for remdesivir, while the SI is 80 for Isopetasin and 50 for neopetasin when tested against the Wuhan virus variant. Interestingly, petasin had the lowest SI value. It is noteworthy to mention that, compared to remdesivir, Ze 339, as well as isopetasin and neopetasin, exerted a higher selectivity index. This is very important since a vast majority of drug candidates, including repurposed drugs, currently evaluated as COVID-19 treatments, have SIs that are much lower than that achieved by Ze 339 or the petasines [57].

3.2. Inhibition Assay of Remdesivir, Ze 339 and Isopetasin against the SARS-CoV-2 Delta Variant

As novel SARS-CoV-2 variants of clinical concern spontaneously develop around the world, we tested the antiviral activity of Ze 339 and isopetasin also against the currently dominant SARS-CoV-2 Delta variant. In a first proof-of-concept experiment, the effect of Ze 339, as well as isopetasin, was investigated in the plaque reduction assay when added to the cells prior to infection with the Delta variant. For this experiment, only isopetasin was chosen out of the petasins since it is the most stable isomer and exerts the lowest IC_{50} value when tested against the Wuhan variant. After infection of Vero E6 cells with the Delta virus variant, Ze 339 showed a slightly lower antiviral activity with an IC_{50} of 0.40 µg/mL and isopetasin with an IC_{50} of 0.28 µg/mL (0.88 µM) (Figure 4). A comparable SARS-CoV-2 inhibitory activity of isopetasin and remdesivir against the Delta variant was observed in this infection experiment. When compared to the Wuhan variant, the activity of Ze 339 and isopetasin against the Delta variant was comparable.

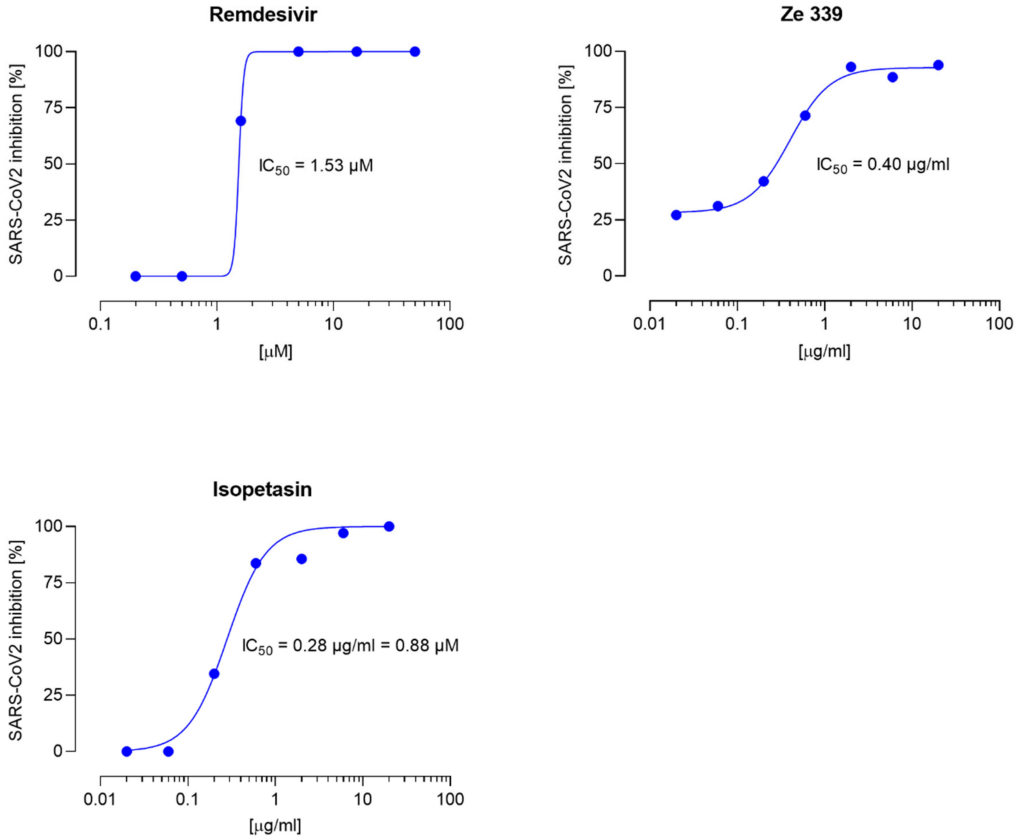

Figure 4. Dose response curves for remdesivir, Ze 339, and isopetasin on the SARS-CoV-2 Delta variant. Cells were infected with 100 pfu of a clinical virus isolate in the presence of the indicated

concentrations. Blue circles represent inhibition of SARS-CoV-2 infection (%). Data are expressed as the mean of duplicate measurements with their respected 95% confidence interval. Ze 339: 95% confidence interval 0.26–0.58, goodness of fit = 0.9943; isopetasin: 95% confidence interval = 0.21–0.38, goodness of fit = 0.9845.

4. Discussion

In facing a rapidly expanding new disease such as COVID-19, drug repurposing of existing moieties appears to be a very favorable approach as their development process to drug approval can utilize pre-existing preclinical and often clinical or post-marketing data [55,58].

The current study demonstrates that Ze 339, isopetasin, as well as neopetasin were able to potently protect cells from SARS-CoV-2 infection. The antiviral activity of Ze 339 (IC_{50} 0.10 µg/mL) against the initial Wuhan strain clearly exceeded that of remdesivir (IC_{50} 1.42 µg/mL). Similar potencies were observed for the Delta variant, while Ze 339 protected cells from an SARS-CoV-2_D infection with an IC_{50} of 0.40 µg/mL (remdesivir: IC_{50} of 0.91 µg/mL). The experiments with isolated petasins suggest that the antiviral effect of Ze 339 is due to the sum of petasins.

Easy-to-use and affordable COVID-19 therapies are urgently needed for clinical disease management. A great advantage of Ze 339, therefore, is that it already is an approved OTC drug in Switzerland, and various other countries for oral treatment of seasonal allergic rhinitis. Further, Ze 339 is available for self-medication. Clinical and post-marketing surveillance studies did not reveal any safety concerns [59–63]. The range and incidence of adverse effects in the respective studies were very low, and described adverse events had all previously been known and are included in the summary of product characteristics [64]. Furthermore, as an approved drug, Ze 339 is subject to pharmacovigilance activities according to current standard procedures. The lack of safety findings reported for *P. hybridus* extract Ze 339 reflects the fairly robust overall safety assessment from clinical experience exceeding 15 years since marketing authorization.

In addition, the mechanism of action as well as the active compounds of Ze 339 were well-described. From a range of pharmacological studies, Ze 339 and its active constituents, petasin, and its isomers, iso- and neopetasin, were shown to ultimately inhibit the synthesis of leukotrienes in human target cells, such as leukocytes and macrophages cultured in vitro or ex vivo [39–41,65]. Moreover, Ze 339 has been shown to reduce TNF-α, IL-6, and IL-8 levels in human nasal epithelial cells challenged with viral mimetics [42].

Furthermore, in addition to the above-mentioned mechanisms of action, petasin is also a potent activator of the AMP-activated protein kinase (AMPK) [66]. AMPK impairs SARS-CoV-2 replication in several ways. It activates AMPK phosphorylates angiotensin-converting enzyme 2 and decreases SARS-CoV-2 binding to the enzyme, thereby decreasing cellular uptake of the virus [67]. Activated AMPK also suppresses the protein kinase B (AKT)/mechanistic target of the rapamycin (mTOR) pathway, which is required for viral protein translation and replication [68]. This is consistent with previous clinical data showing an improved mortality in diabetic COVID-19 patients treated with the indirect AMPK activator metformin [69–71]. Finally, metformin suppresses inflammatory pathways and immunological responses (cytokine storms) [72].

It is also worth mentioning that the mechanism of anti-inflammatory action of Ze 339 is comparable to that of montelukast and zileuton, which are currently under discussion as therapeutic candidates for the treatment of COVID-19 [25–29]. A recent study by Durdagi et al. [73] demonstrated that the neutralization effect of montelukast on SARS-CoV-2 in vitro suggests that virus replication could be significantly delayed. The authors suggested to consider montelukast for prophylactic treatment. In our current study, a pre-incubation of cells with the test compounds for 2 h prior to virus infection had a clear positive effect, suggesting a possible prophylactic role also for the petasins. While the montelukast IC_{50} values were at 18.82 µM and 25 µM in in vitro cell culture models of SARS-CoV-2 activity [73,74], the IC_{50}s for Ze 339, isopetasin, and neopetasin determined in the current

study were significantly lower. The visibly shallower inhibition curves of the petasin compounds compared to the antiviral mechanism of remdesivir could suggest a more complex mode of interference with the viral life cycle which is supported by the above-mentioned various mechanisms of action of Ze 339. A similar difference is also observed for different HIV inhibitor classes (e.g., nucleosidic polymerase inhibitors versus protease inhibitors, which are not shown).

Furthermore, it is worth mentioning that the three petasin isomers meet all criteria of druglikeness, such as Lipinski's '*rule of five*' [75], as well as the criteria of Ghoose [76] and Veber [77], which are all recognized predictors of good oral bioavailability, as shown in Table S1, Supporting Information. Currently, the molecular mechanism by which the petasin isomers exert their antiviral effects can only be speculated about. However, Kc and colleagues recently presented a method utilizing machine learning to estimate aspects of antiviral activity also covering mechanisms (http://drugcentral.org/Redial (accessed on 1 December 2021)) [78]. The platform uses validated machine learning models to generate predictions based on user's SMILES input from their compounds of interest. The petasin isomers were tested in this platform (data are shown in Supplemenatry Figure S2, Supporting Information) and yielded predictions of activity on receptor binding (*Spike-ACE2 protein-protein interaction* (*AlphaLISA*)) and viral replication (*3CL enzymatic activity*) for petasin and neopetasin, as well as for the inhibition of viral entry for isopetasin only (*Spike-ACE2 protein-protein interaction* (*AlphaLISA*)). All isomers were predicted negative for human cell toxicity. While these data are interesting, a definite proof will require further details in in vitro studies.

5. Conclusions

In conclusion, since affordable therapies for treating SARS-CoV-2 infection and COVID-19 are urgently needed, we propose that Ze 339 could be a promising candidate for drug repurposing with a supposed dual mode of action through a direct anti-SARS-CoV2 effect and a potent indirect inhibitory effect on leukotriene biosynthesis/cytokine activity or AMPK activation.

Taken together, the *Petasites hybridus* subcritical CO_2 extract, Ze 339, may provide a safe, low-cost alternative for treating patients infected with SARS-CoV-2. As Ze 339 is registered in Switzerland as an OTC drug, it is a promising repurposing candidate due to its proven safety profile. For further development, the current in vitro data will have to be verified in vivo, and a clinical benefit of Ze 339 as a possible drug for treating mild to moderate cases of COVID-19 needs to be proven in future clinical studies.

Supplementary Materials: The following are available online at https://www.mdpi.com/article/10.3390/v14010106/s1, Figure S1: Gas chromatogram of Petasites hybridus leaf extract Ze 339 (batch 150056), Figure S2. Prediction of anti-viral mechanisms (a) Petasin (b) Isopetasin, Table S1: Druglikeness of petasin, isopetasin and neopetasin.

Author Contributions: Conceptualization, T.K., M.H.K., V.B. and J.D.; methodology, L.U.; software L.U. and V.B.; formal analysis, V.B. and G.B.; writing—original draft preparation, V.B., G.B. and T.K.; writing—review and editing, J.D.; visualization, V.B.; supervision, T.K. All authors have read and agreed to the published version of the manuscript.

Funding: The study was funded by Max Zeller Soehne AG, CH-8590 Romanshorn, Switzerland.

Institutional Review Board Statement: Not applicable.

Informed Consent Statement: Not applicable.

Data Availability Statement: Data are available on request from the authors.

Acknowledgments: For providing access to the SARS-CoV-2 strain/NL/2020—AMS, we thank the EVA GLOBAL consortium (funded by the European Union's Horizon 2020 research and innovation programme under grant agreement No. 871029) and B. Hagman (https://www.european-virus-archive.com/virus/sars-cov-2-strain-nl2020 (accessed on 1 December 2021)).

Conflicts of Interest: M.H.K., V.B., J.D. and G.B. are employees of Max Zeller Soehne AG, CH-8590 Romanshorn, Switzerland, the manufacturer of Ze 339.

References

1. Coronavirus Resource Center. COVID-19 Dashboard by the Center for Systems Science and Engineering (CSSE) at Johns Hopkins University (JHU). Available online: https://coronavirus.jhu.edu/map.html (accessed on 1 December 2021).
2. Tizaoui, K.; Zidi, I.; Lee, K.H.; Ghayda, R.A.; Hong, S.H.; Li, H.; Smith, L.; Koyanagi, A.; Jacob, L.; Kronbichler, A.; et al. Update of the current knowledge on genetics, evolution, immunopathogenesis, and transmission for coronavirus disease 19 (COVID-19). *Int. J. Biol. Sci.* **2020**, *16*, 2906–2923. [CrossRef] [PubMed]
3. England, J.T.; Abdulla, A.; Biggs, C.M.; Lee, A.Y.Y.; Hay, K.A.; Hoiland, R.L.; Wellington, C.L.; Sekhon, M.; Jamal, S.; Shojania, K.; et al. Weathering the COVID-19 storm: Lessons from hematologic cytokine syndromes. *Blood Rev.* **2021**, *45*, 100707. [CrossRef] [PubMed]
4. Qin, C.; Zhou, L.; Hu, Z.; Zhang, S.; Yang, S.; Tao, Y.; Xie, C.; Ma, K.; Shang, K.; Wang, W.; et al. Dysregulation of Immune Response in Patients With Coronavirus 2019 (COVID-19) in Wuhan, China. *Clin. Infect. Dis* **2020**, *71*, 762–768. [CrossRef] [PubMed]
5. Clark, I.A. The advent of the cytokine storm. *Immunol. Cell Biol.* **2007**, *85*, 271–273. [CrossRef]
6. Jose, R.J.; Manuel, A. COVID-19 cytokine storm: The interplay between inflammation and coagulation. *Lancet Respir. Med.* **2020**, *8*, e46–e47. [CrossRef]
7. Carsana, L.; Sonzogni, A.; Nasr, A.; Rossi, R.S.; Pellegrinelli, A.; Zerbi, P.; Rech, R.; Colombo, R.; Antinori, S.; Corbellino, M.; et al. Pulmonary post-mortem findings in a series of COVID-19 cases from northern Italy: A two-centre descriptive study. *Lancet Infect. Dis.* **2020**, *20*, 1135–1140. [CrossRef]
8. Grasselli, G.; Tonetti, T.; Protti, A.; Langer, T.; Girardis, M.; Bellani, G.; Laffey, J.; Carrafiello, G.; Carsana, L.; Rizzuto, C.; et al. Pathophysiology of COVID-19-associated acute respiratory distress syndrome: A multicentre prospective observational study. *Lancet Respir. Med.* **2020**, *8*, 1201–1208. [CrossRef]
9. Sonzogni, A.; Previtali, G.; Seghezzi, M.; Grazia Alessio, M.; Gianatti, A.; Licini, L.; Morotti, D.; Zerbi, P.; Carsana, L.; Rossi, R.; et al. Liver histopathology in severe COVID 19 respiratory failure is suggestive of vascular alterations. *Liver Int.* **2020**, *40*, 2110–2116. [CrossRef]
10. Maiuolo, J.; Mollace, R.; Gliozzi, M.; Musolino, V.; Carresi, C.; Paone, S.; Scicchitano, M.; Macri, R.; Nucera, S.; Bosco, F.; et al. The Contribution of Endothelial Dysfunction in Systemic Injury Subsequent to SARS-Cov-2 Infection. *Int. J. Mol. Sci.* **2020**, *21*, 9309. [CrossRef]
11. Combes, A.J.; Courau, T.; Kuhn, N.F.; Hu, K.H.; Ray, A.; Chen, W.S.; Chew, N.W.; Cleary, S.J.; Kushnoor, D.; Reeder, G.C.; et al. Global absence and targeting of protective immune states in severe COVID-19. *Nature* **2021**, *591*, 124–130. [CrossRef]
12. Rodriguez, C.; Luque, N.; Blanco, I.; Sebastian, L.; Barbera, J.A.; Peinado, V.I.; Tura-Ceide, O. Pulmonary Endothelial Dysfunction and Thrombotic Complications in Patients with COVID-19. *Am. J. Respir. Cell Mol. Biol.* **2021**, *64*, 407–415. [CrossRef]
13. Yang, L.; Xie, X.; Tu, Z.; Fu, J.; Xu, D.; Zhou, Y. The signal pathways and treatment of cytokine storm in COVID-19. *Signal. Transduct Target. Ther.* **2021**, *6*, 255. [CrossRef]
14. Couzin-Frankel, J. Antiviral pills could change pandemic's course. *Science* **2021**, *374*, 799–800. [CrossRef]
15. Xiong, M.; Su, H.; Zhao, W.; Xie, H.; Shao, Q.; Xu, Y. What coronavirus 3C-like protease tells us: From structure, substrate selectivity, to inhibitor design. *Med. Res. Rev.* **2021**, *41*, 1965–1998. [CrossRef]
16. Pfizer Pfizer Press Release: Pfizer Initiates Phase 1 Study of Novel Oral Antiviral Therapeutic Agent Against SARS-COV-2. Available online: https://www.pfizer.com/news/press-release/press-release-detail/pfizer-initiates-phase-1-study-novel-oral-antiviral (accessed on 30 November 2021).
17. Group, R.C.; Horby, P.; Lim, W.S.; Emberson, J.R.; Mafham, M.; Bell, J.L.; Linsell, L.; Staplin, N.; Brightling, C.; Ustianowski, A.; et al. Dexamethasone in Hospitalized Patients with Covid-19. *N. Engl. J. Med.* **2021**, *384*, 693–704. [CrossRef]
18. Mahase, E. Covid-19: Demand for dexamethasone surges as RECOVERY trial publishes preprint. *BMJ* **2020**, *369*, m2512. [CrossRef] [PubMed]
19. Olender, S.A.; Perez, K.K.; Go, A.S.; Balani, B.; Price-Haywood, E.G.; Shah, N.S.; Wang, S.; Walunas, T.L.; Swaminathan, S.; Slim, J.; et al. Remdesivir for Severe COVID-19 versus a Cohort Receiving Standard of Care. *Clin. Infect. Dis.* **2020**, *73*, e4166–e4174. [CrossRef]
20. Olender, S.A.; Walunas, T.L.; Martinez, E.; Perez, K.K.; Castagna, A.; Wang, S.; Kurbegov, D.; Goyal, P.; Ripamonti, D.; Balani, B.; et al. Remdesivir Versus Standard-of-Care for Severe Coronavirus Disease 2019 Infection: An Analysis of 28-Day Mortality. *Open Forum Infect. Dis.* **2021**, *8*, ofab278. [CrossRef]

21. Spinner, C.D.; Gottlieb, R.L.; Criner, G.J.; Arribas Lopez, J.R.; Cattelan, A.M.; Soriano Viladomiu, A.; Ogbuagu, O.; Malhotra, P.; Mullane, K.M.; Castagna, A.; et al. Effect of Remdesivir vs Standard Care on Clinical Status at 11 Days in Patients With Moderate COVID-19: A Randomized Clinical Trial. *JAMA* **2020**, *324*, 1048–1057. [CrossRef]
22. Wang, L.Y.; Cui, J.J.; Ouyang, Q.Y.; Zhan, Y.; Guo, C.X.; Yin, J.Y. Remdesivir and COVID-19. *Lancet* **2020**, *396*, 953–954. [CrossRef]
23. Wang, Y.; Zhang, D.; Du, G.; Du, R.; Zhao, J.; Jin, Y.; Fu, S.; Gao, L.; Cheng, Z.; Lu, Q.; et al. Remdesivir in adults with severe COVID-19: A randomised, double-blind, placebo-controlled, multicentre trial. *Lancet* **2020**, *395*, 1569–1578. [CrossRef]
24. Wang, Y.; Zhou, F.; Zhang, D.; Zhao, J.; Du, R.; Hu, Y.; Cheng, Z.; Gao, L.; Jin, Y.; Luo, G.; et al. Evaluation of the efficacy and safety of intravenous remdesivir in adult patients with severe COVID-19: Study protocol for a phase 3 randomized, double-blind, placebo-controlled, multicentre trial. *Trials* **2020**, *21*, 422. [CrossRef] [PubMed]
25. Almerie, M.Q.; Kerrigan, D.D. The association between obesity and poor outcome after COVID-19 indicates a potential therapeutic role for montelukast. *Med. Hypotheses* **2020**, *143*, 109883. [CrossRef]
26. Bozek, A.; Winterstein, J. Montelukast's ability to fight COVID-19 infection. *J. Asthma* **2021**, *58*, 1348–1349. [CrossRef]
27. Funk, C.D.; Ardakani, A. A Novel Strategy to Mitigate the Hyperinflammatory Response to COVID-19 by Targeting Leukotrienes. *Front. Pharmacol.* **2020**, *11*, 1214. [CrossRef]
28. Fidan, C.; Aydogdu, A. As a potential treatment of COVID-19: Montelukast. *Med. Hypotheses* **2020**, *142*, 109828. [CrossRef]
29. Citron, F.; Perelli, L.; Deem, A.K.; Genovese, G.; Viale, A. Leukotrienes, a potential target for Covid-19. *Prostaglandins Leukot. Essent. Fat. Acids* **2020**, *161*, 102174. [CrossRef]
30. Archambault, A.S.; Zaid, Y.; Rakotoarivelo, V.; Turcotte, C.; Dore, E.; Dubuc, I.; Martin, C.; Flamand, O.; Amar, Y.; Cheikh, A.; et al. High levels of eicosanoids and docosanoids in the lungs of intubated COVID-19 patients. *FASEB J.* **2021**, *35*, e21666. [CrossRef]
31. Zaid, Y.; Dore, E.; Dubuc, I.; Archambault, A.S.; Flamand, O.; Laviolette, M.; Flamand, N.; Boilard, E.; Flamand, L. Chemokines and eicosanoids fuel the hyperinflammation within the lungs of patients with severe COVID-19. *J. Allergy Clin. Immunol.* **2021**, *148*, 368–380.e3. [CrossRef]
32. Funk, C.D. Prostaglandins and leukotrienes: Advances in eicosanoid biology. *Science* **2001**, *294*, 1871–1875. [CrossRef]
33. Kanaoka, Y.; Boyce, J.A. Cysteinyl leukotrienes and their receptors: Cellular distribution and function in immune and inflammatory responses. *J. Immunol.* **2004**, *173*, 1503–1510. [CrossRef]
34. Werz, O.; Steinhilber, D. Therapeutic options for 5-lipoxygenase inhibitors. *Pharmacol. Ther.* **2006**, *112*, 701–718. [CrossRef]
35. Sharma, J.N.; Mohammed, L.A. The role of leukotrienes in the pathophysiology of inflammatory disorders: Is there a case for revisiting leukotrienes as therapeutic targets? *Inflammopharmacology* **2006**, *14*, 10–16. [CrossRef]
36. Singh, R.K.; Tandon, R.; Dastidar, S.G.; Ray, A. A review on leukotrienes and their receptors with reference to asthma. *J. Asthma* **2013**, *50*, 922–931. [CrossRef]
37. Brattström, A. A newly developed extract (Ze 339) from butterbur (Petasites hybridus L.) is clinically efficient in allergic rhinitis (hay fever). *Phytomedicine* **2003**, *10*, 50–52. [CrossRef]
38. Kodjadjiku, U.; Nagele, B.; Halbsguth, C.; Butterweck, V. Extract matrix composition does not affect in vitro leukotriene inhibitory effects of the Petasites hybridus extract Ze 339. *Fitoterapia* **2021**, *153*, 104986. [CrossRef]
39. Thomet, O.A.; Schapowal, A.; Heinisch, I.V.; Wiesmann, U.N.; Simon, H.U. Anti-inflammatory activity of an extract of Petasites hybridus in allergic rhinitis. *Int. Immunopharmacol.* **2002**, *2*, 997–1006. [CrossRef]
40. Thomet, O.A.; Wiesmann, U.N.; Blaser, K.; Simon, H.U. Differential inhibition of inflammatory effector functions by petasin, isopetasin and neopetasin in human eosinophils. *Clin. Exp. Allergy* **2001**, *31*, 1310–1320. [CrossRef]
41. Thomet, O.A.R.; Wiesmann, U.N.; Schapowal, A.; Bizer, C.; Simon, H.-U. Role of petasin in the potential anti-inflammatory activity of a plant extract of petasites hybridus. *Biochem. Pharmacol.* **2001**, *61*, 1041–1047. [CrossRef]
42. Steiert, S.A.; Zissler, U.M.; Chaker, A.M.; Esser-von-Bieren, J.; Dittlein, D.; Guerth, F.; Jakwerth, C.A.; Piontek, G.; Zahner, C.; Drewe, J.; et al. Anti-inflammatory effects of the petasin phyto drug Ze339 are mediated by inhibition of the STAT pathway. *Biofactors* **2017**, *43*, 388–399. [CrossRef]
43. Koch, V.; Rittinghausen, R. Composition Containing Pyrrolizidine-Alkaloid-Free Petasites. US Patent US6551626B1, 22 April 2003.
44. Steiner, R.; Hauk, A.; Tratz, W. Method for Producing Medicinal Plant Extracts. International Patent WO/1999/018984, 29 April 1999.
45. Corman, V.M.; Landt, O.; Kaiser, M.; Molenkamp, R.; Meijer, A.; Chu, D.K.; Bleicker, T.; Brunink, S.; Schneider, J.; Schmidt, M.L.; et al. Detection of 2019 novel coronavirus (2019-nCoV) by real-time RT-PCR. *Euro Surveill.* **2020**, *25*, 2000045. [CrossRef] [PubMed]
46. Honko, A.N.; Storm, N.; Bean, D.J.; Henao Vasquez, J.; Downs, S.N.; Griffiths, A. Rapid Quantification and Neutralization Assays for Novel Coronavirus SARS-CoV-2 Using Avicel RC-591 Semi-Solid Overlay. *Preprints* **2020**, 2020050264. [CrossRef]
47. Rasband, W.S. Image J. Available online: https://imagej.nih.gov/ij/ (accessed on 2 October 2021).
48. Baer, A.; Kehn-Hall, K. Viral concentration determination through plaque assays: Using traditional and novel overlay systems. *J. Vis. Exp.* **2014**, e52065. [CrossRef] [PubMed]
49. Wu, C.Y.; Jan, J.T.; Ma, S.H.; Kuo, C.J.; Juan, H.F.; Cheng, Y.S.; Hsu, H.H.; Huang, H.C.; Wu, D.; Brik, A.; et al. Small molecules targeting severe acute respiratory syndrome human coronavirus. *Proc. Natl. Acad. Sci. USA* **2004**, *101*, 10012–10017. [CrossRef]
50. Ao, Z.; Chan, M.; Ouyang, M.J.; Olukitibi, T.A.; Mahmoudi, M.; Kobasa, D.; Yao, X. Identification and evaluation of the inhibitory effect of Prunella vulgaris extract on SARS-coronavirus 2 virus entry. *PLoS ONE* **2021**, *16*, e0251649. [CrossRef]
51. Jeon, S.; Ko, M.; Lee, J.; Choi, I.; Byun, S.Y.; Park, S.; Shum, D.; Kim, S. Identification of Antiviral Drug Candidates against SARS-CoV-2 from FDA-Approved Drugs. *Antimicrob. Agents Chemother.* **2020**, *64*, e00819-20. [CrossRef]

52. Ku, K.B.; Shin, H.J.; Kim, H.S.; Kim, B.T.; Kim, S.J.; Kim, C. Repurposing Screens of FDA-Approved Drugs Identify 29 Inhibitors of SARS-CoV-2. *J. Microbiol. Biotechnol.* **2020**, *30*, 1843–1853. [CrossRef]
53. Matsuyama, S.; Nao, N.; Shirato, K.; Kawase, M.; Saito, S.; Takayama, I.; Nagata, N.; Sekizuka, T.; Katoh, H.; Kato, F.; et al. Enhanced isolation of SARS-CoV-2 by TMPRSS2-expressing cells. *Proc. Natl. Acad. Sci. USA* **2020**, *117*, 7001–7003. [CrossRef]
54. Tietjen, I.; Cassel, J.; Register, E.T.; Zhou, X.Y.; Messick, T.E.; Keeney, F.; Lu, L.D.; Beattie, K.D.; Rali, T.; Tebas, P.; et al. The natural stilbenoid (-)-hopeaphenol inhibits cellular entry of SARS-CoV-2 USA-WA1/2020, B.1.1.7 and B.1.351 variants. *Antimicrob. Agents Chemother.* **2021**, *65*, AAC0077221. [CrossRef]
55. Ellinger, B.; Bojkova, D.; Zaliani, A.; Cinatl, J.; Claussen, C.; Westhaus, S.; Keminer, O.; Reinshagen, J.; Kuzikov, M.; Wolf, M.; et al. A SARS-CoV-2 cytopathicity dataset generated by high-content screening of a large drug repurposing collection. *Sci. Data* **2021**, *8*, 70. [CrossRef]
56. Indrayanto, G.; Putra, G.S.; Suhud, F. Validation of in-vitro bioassay methods: Application in herbal drug research. *Profiles Drug Subst. Excip. Relat. Methodol.* **2021**, *46*, 273–307. [CrossRef]
57. GHDDI Info Sharing Portal. COVID-19 Preclinical Studies. Available online: https://ghddi-ailab.github.io/Targeting2019-nCoV/preclinical/ (accessed on 20 November 2021).
58. Dittmar, M.; Lee, J.S.; Whig, K.; Segrist, E.; Li, M.; Kamalia, B.; Castellana, L.; Ayyanathan, K.; Cardenas-Diaz, F.L.; Morrisey, E.E.; et al. Drug repurposing screens reveal cell-type-specific entry pathways and FDA-approved drugs active against SARS-Cov-2. *Cell Rep.* **2021**, *35*, 108959. [CrossRef]
59. Blosa, M.; Uricher, J.; Nebel, S.; Zahner, C.; Butterweck, V.; Drewe, J. Treatment of Early Allergic and Late Inflammatory Symptoms of Allergic Rhinitis with Petasites hybridus Leaf Extract (Ze 339): Results of a Noninterventional Observational Study in Switzerland. *Pharmaceuticals* **2021**, *14*, 180. [CrossRef]
60. Dumitru, A.F.; Shamji, M.; Wagenmann, M.; Hindersin, S.; Scheckenbach, K.; Greve, J.; Klenzner, T.; Hess, L.; Nebel, S.; Zimmermann, C.; et al. Petasol butenoate complex (Ze 339) relieves allergic rhinitis-induced nasal obstruction more effectively than desloratadine. *J. Allergy Clin. Immunol.* **2011**, *127*, 1515–1521. [CrossRef]
61. Schapowal, A.; Petasites Study, G. Randomised controlled trial of butterbur and cetirizine for treating seasonal allergic rhinitis. *BMJ* **2002**, *324*, 144–146. [CrossRef]
62. Schapowal, A.; Petasites Study, G. Butterbur Ze339 for the treatment of intermittent allergic rhinitis: Dose-dependent efficacy in a prospective, randomized, double-blind, placebo-controlled study. *Arch. Otolaryngol. Head Neck Surg.* **2004**, *130*, 1381–1386. [CrossRef]
63. Schapowal, A.; Study Group. Treating intermittent allergic rhinitis: A prospective, randomized, placebo and antihistamine-controlled study of Butterbur extract Ze 339. *Phytother. Res.* **2005**, *19*, 530–537. [CrossRef]
64. Product Information. Available online: https://www.swissmedicinfo.ch/?Lang=EN (accessed on 1 December 2021).
65. Thomet, O.A.; Simon, H.U. Petasins in the treatment of allergic diseases: Results of preclinical and clinical studies. *Int. Arch. Allergy Immunol.* **2002**, *129*, 108–112. [CrossRef]
66. Adachi, Y.; Kanbayashi, Y.; Harata, I.; Ubagai, R.; Takimoto, T.; Suzuki, K.; Miwa, T.; Noguchi, Y. Petasin activates AMP-activated protein kinase and modulates glucose metabolism. *J. Nat. Prod.* **2014**, *77*, 1262–1269. [CrossRef]
67. Sharma, S.; Ray, A.; Sadasivam, B. Metformin in COVID-19: A possible role beyond diabetes. *Diabetes Res. Clin. Pract.* **2020**, *164*, 108183. [CrossRef]
68. Karam, B.S.; Morris, R.S.; Bramante, C.T.; Puskarich, M.; Zolfaghari, E.J.; Lotfi-Emran, S.; Ingraham, N.E.; Charles, A.; Odde, D.J.; Tignanelli, C.J. mTOR inhibition in COVID-19: A commentary and review of efficacy in RNA viruses. *J. Med. Virol.* **2021**, *93*, 1843–1846. [CrossRef]
69. Kow, C.S.; Hasan, S.S. Mortality risk with preadmission metformin use in patients with COVID-19 and diabetes: A meta-analysis. *J. Med. Virol.* **2021**, *93*, 695–697. [CrossRef]
70. Lally, M.A.; Tsoukas, P.; Halladay, C.W.; O'Neill, E.; Gravenstein, S.; Rudolph, J.L. Metformin is Associated with Decreased 30-Day Mortality Among Nursing Home Residents Infected with SARS-CoV2. *J. Am. Med. Dir. Assoc.* **2021**, *22*, 193–198. [CrossRef]
71. Nafakhi, H.; Alareedh, M.; Al-Buthabhak, K.; Shaghee, F.; Nafakhi, A.; Kasim, S. Predictors of adverse in-hospital outcome and recovery in patients with diabetes mellitus and COVID-19 pneumonia in Iraq. *Diabetes Metab Syndr.* **2021**, *15*, 33–38. [CrossRef]
72. Chen, X.; Guo, H.; Qiu, L.; Zhang, C.; Deng, Q.; Leng, Q. Immunomodulatory and Antiviral Activity of Metformin and Its Potential Implications in Treating Coronavirus Disease 2019 and Lung Injury. *Front. Immunol.* **2020**, *11*, 2056. [CrossRef]
73. Durdagi, S.; Avsar, T.; Orhan, M.D.; Serhatli, M.; Balcioglu, B.K.; Ozturk, H.U.; Kayabolen, A.; Cetin, Y.; Aydinlik, S.; Bagci-Onder, T.; et al. The neutralization effect of montelukaston SARS-CoV-2 is shown by multiscale in silicosimulations and combined in vitro studies. *Mol. Ther.* **2021**, *30*, 1–12. [CrossRef]
74. Kumar, S.; Singh, B.; Kumari, P.; Kumar, P.V.; Agnihotri, G.; Khan, S.; Kant Beuria, T.; Syed, G.H.; Dixit, A. Identification of multipotent drugs for COVID-19 therapeutics with the evaluation of their SARS-CoV2 inhibitory activity. *Comput. Struct. Biotechnol. J.* **2021**, *19*, 1998–2017. [CrossRef]
75. Lipinski, C.A.; Lombardo, F.; Dominy, B.W.; Feeney, P.J. Experimental and computational approaches to estimate solubility and permeability in drug discovery and development settings. *Adv. Drug Deliv. Rev.* **2001**, *46*, 3–26. [CrossRef]
76. Ghose, A.K.; Viswanadhan, V.N.; Wendoloski, J.J. A knowledge-based approach in designing combinatorial or medicinal chemistry libraries for drug discovery. 1. A qualitative and quantitative characterization of known drug databases. *J. Comb. Chem.* **1999**, *1*, 55–68. [CrossRef] [PubMed]

77. Veber, D.F.; Johnson, S.R.; Cheng, H.Y.; Smith, B.R.; Ward, K.W.; Kopple, K.D. Molecular properties that influence the oral bioavailability of drug candidates. *J. Med. Chem.* **2002**, *45*, 2615–2623. [CrossRef] [PubMed]
78. KC, G.B.; Bocci, G.; Verma, S.; Hassan, M.; Holmes, J.; Yang, J.J.; Sirimulla, S.; Oprea, T.I. A machine learning platform to estimate anti-SARS-CoV-2 activities. *Nat. Mach. Intell.* **2021**, *3*, 527–535. [CrossRef]